

# Investigating Local Structure in Layered Double Hydroxides with $^{17}\text{O}$ NMR Spectroscopy

Li Zhao, Zhe Qi, Frédéric Blanc, Guiyun Yu, Meng Wang, Nianhua Xue, Xiaokang Ke, Xuefeng Guo, Weiping Ding, Clare P. Grey, and Luming Peng\*

A new method based on the “memory effect” for efficient and economical  $^{17}\text{O}$  labeling of layered double hydroxides (LDHs) is introduced. High-quality  $^{17}\text{O}$  solid-state NMR spectra are obtained, for the first time, for LDHs prepared with only several hundred microliters of  $^{17}\text{O}$ -enriched  $\text{H}_2\text{O}$ . The  $^{17}\text{O}$  resonances due to the different oxygen ions in the structure of LDHs can be resolved with better resolution than the results obtained from  $^1\text{H}$  ultrafast magic angle spinning (MAS) NMR spectroscopy. The results show clear evidence for Al–O–Al avoidance. Since only intermediate MAS speeds and fields are used, this new approach can be incorporated easily with a variety of dipolar recoupling schemes to explore the key interactions and applications of LDHs.

## 1. Introduction

Layered double hydroxides (LDHs), or “hydrotalcite-type” materials, possess the general formula  $\text{M}^{2+}_{1-x}\text{M}^{3+}_x(\text{OH})_2(\text{A}^{n-})_{x/n} \cdot y\text{H}_2\text{O}$ , where a fraction ( $x\%$ , where  $x$  varies from 17 to 33%) of divalent metal cations  $\text{M}^{2+}$ , for example,  $\text{Mg}^{2+}$ , located in a brucite-like environment are substituted by trivalent  $\text{M}^{3+}$ , for example,  $\text{Al}^{3+}$ , cations. This results in positively-charged metal hydroxide layers with charge compensating and exchangeable anions ( $\text{A}^{n-}$ ) and water molecules between the layers (Figure 1).<sup>[1,2]</sup> LDHs are important inorganic supramolecular compounds that can be designed to incorporate a variety of cations and anions and used as precursors for many functional mixed oxides. They have, therefore, received considerable attention in a wide range of applications including but not limited to, optical devices,<sup>[3,4]</sup> catalysis,<sup>[5]</sup> environmental management,<sup>[6,7]</sup> and biological sciences.<sup>[8–10]</sup> The rational design of LDHs with targeted properties relies on knowledge of the  $\text{M}^{2+}/\text{M}^{3+}$  intralayer cation ordering and the supramolecular host-guest interactions between the hydroxide layer cations and the anions in the interlayer

regions.<sup>[11]</sup> Despite this, compelling evidence for cation local ordering is only just starting to emerge.<sup>[12–15]</sup>

Solid-state NMR spectroscopy is a powerful tool with which to probe local environments on an atomic length scale. Although  $^{27}\text{Al}$  magic angle spinning (MAS) NMR experiments have long been used to track Al coordination changes on thermal treatment of LDHs, they are not sensitive to intralayer cation distributions.<sup>[16]</sup> More recently, Sideris and co-workers showed that solid state  $^1\text{H}$  NMR spectroscopy coupled with very fast magic angle spinning (MAS) could be used to resolve and quantify the signals

originating from both  $\text{Mg}_3\text{OH}$  and  $\text{Mg}_2\text{AlOH}$  environments (Figure 1c).<sup>[15]</sup> The  $^1\text{H}$  NMR results showed a non-random Mg/Al distribution and the avoidance of Al–O–Al linkages, leading to a “honeycomb” ordering of 33% Al substituted material. Cadars et al. then argued based on their  $^1\text{H}$  double quantum (DQ) MAS NMR spectroscopy results that even within a largely ordered structure, a small concentration of defects, for example,  $\text{MgAl}_2\text{OH}$ , could exist in Al rich LDHs.<sup>[13]</sup> Cation ordering was further supported by the  $^{25}\text{Mg}$  NMR data obtained by Sideris et al. at an ultrahigh magnetic field, where it was argued that the presence of defects in some samples was likely a consequence of the synthesis method.<sup>[14,15]</sup> Large  $^1\text{H}$ – $^1\text{H}$  homonuclear dipolar couplings are present in these systems,<sup>[17]</sup> and ultrafast spinning rates (i.e.,  $>40\text{ kHz}$ )<sup>[18]</sup> were required for the  $\text{NO}_3^-$ -containing LDHs to allow resolution of the major resonances.<sup>[13–15]</sup> With different anions in the interlayer regions, for example, the carbonate ion,  $\text{CO}_3^{2-}$ , however, the resonance becomes much broader and the spectral resolution decreases significantly due to the difficulty in removing larger  $^1\text{H}$ – $^1\text{H}$  homonuclear dipolar coupling and/or chemical exchange between the different proton species.<sup>[14]</sup> Therefore, new approaches are needed to study the local structure of LDHs and perform double resonance experiments to investigate the fundamental interactions between cations and anions that define the supramolecular chemistry in LDHs.

Oxygen is a major component of all LDHs and has the largest ionic radius in the materials, making this nucleus intimately involved in many function-related processes. Oxygen anions in the layer are connected to all of the cations (i.e.,  $\text{M}^{2+}$ ,  $\text{M}^{3+}$ , and  $\text{H}^+$ , Figure 1c) and therefore investigating the structure of LDHs via the oxygen atom is a more direct route to determine the cation ordering, as compared to proton or any

L. Zhao, Z. Qi, G. Yu, M. Wang, Dr. N. Xue, X. Ke, Prof. X. Guo, Prof. W. Ding, Dr. L. Peng  
School of Chemistry and Chemical Engineering  
Nanjing University, 22 Hankou Road  
Nanjing, 210093, China  
E-mail: luming@nju.edu.cn  
Dr. F. Blanc, Prof. C. P. Grey  
Department of Chemistry  
University of Cambridge, Lensfield Road  
Cambridge, CB2 1EW, UK



DOI: 10.1002/adfm.201301157

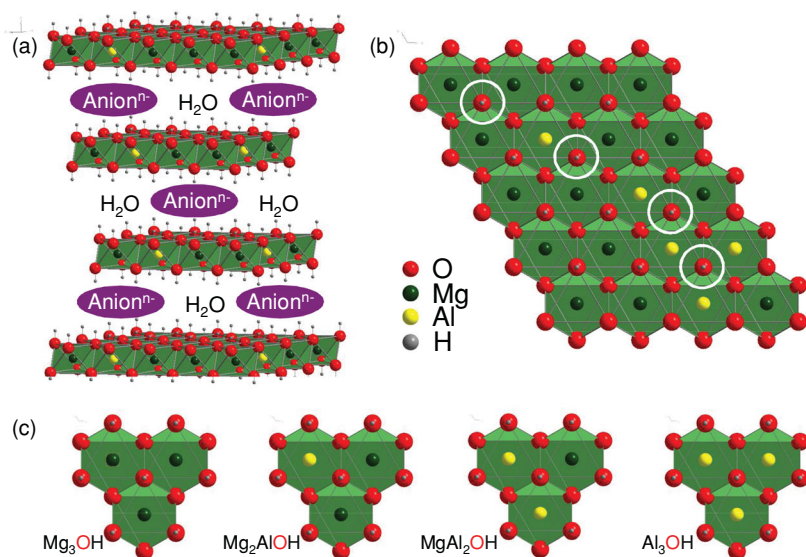


**Figure 1.** a) The schematic representation of the structure of LDH materials with b) random Al distribution and c) the 4 different possible oxygen local environments in the cation layer.

other nucleus. In addition,  $^{17}\text{O}$ , which is the only oxygen NMR active nucleus, is very sensitive to the structural changes due to both a very large chemical shift range of more than 1000 ppm and the quadrupolar interaction (the interaction between the quadrupole moments  $Q$  of the quadrupolar nuclei and the electric field gradient (EFG) generated by their environments) of this spin-5/2 nucleus.<sup>[19]</sup> Therefore  $^{17}\text{O}$  solid-state NMR spectroscopy should be an ideal method with which to study LDHs and provide considerable information not accessible otherwise. To the best of our knowledge, no  $^{17}\text{O}$  NMR spectra of LDHs have been reported, presumably due to the very low natural abundance of  $^{17}\text{O}$  (0.037%) and the issues arising from efficient  $^{17}\text{O}$  isotopic labeling of the materials.<sup>[20]</sup> LDHs are usually prepared with a large amount of water (several hundred mL) as the solvent, incompatible with the use of expensive  $^{17}\text{O}$  enriched water. Herein, we present a highly efficient route for  $^{17}\text{O}$  enrichment of LDHs using the “memory effect”<sup>[1]</sup> requiring only a very small amount (hundreds of  $\mu\text{L}$ ) of  $^{17}\text{O}$  enriched water, and demonstrate how  $^{17}\text{O}$  NMR could be used to investigate the cation ordering in LDHs. The interactions among the interlayer anions, the cations, and water can be investigated in a similar manner.

## 2. Results and Discussion

The LDH samples are designated as “Y- $x$ -An $^-$ ”, where Y stands for the preparation method (“A” = as synthesized, “D” = directly enriched, “M” = enriched via “memory effect”),  $x$  represents the Al mole percentage and “An $^-$ ” shows the interlayer species, respectively (see the Experimental Section for details). The powder XRD patterns of the starting  $\text{CO}_3^{2-}$ -containing LDH materials (Figure S1, Supporting Information) show characteristic diffraction peaks without unwanted phases and the sharp (00 $l$ ) reflections at low  $2\theta$  angles indicate successive orders of basal spacing in LDHs.<sup>[6]</sup> The stoichiometry (Table S1,

Supporting Information) of these layered materials is obtained from ICP spectroscopy in combination with thermogravimetric analysis (Figure S2, Supporting Information).

The one pulse  $^{17}\text{O}$  MAS NMR spectrum of a Mg and Al containing LDH with  $\text{CO}_3^{2-}$  anions in the interlayer regions (D-26.1- $\text{CO}_3^{2-}$ ) prepared by direct  $^{17}\text{O}$  enrichment of the LDH by exchange with  $^{17}\text{O}$ -enriched water is shown in the bottom of Figure 2. Despite a long acquisition time (>2 h), the signal/noise (S/N) ratio remains extremely low and only broad and featureless peaks (at  $\approx 110$  to 20 ppm and 0 to  $-200$  ppm) could be observed from which little structural information could be extracted. Although not successful for efficient  $^{17}\text{O}$  enrichment, this method can be used to track the signal from water in the interlayer regions (see Figure S3 and other Supporting Information).

LDHs are known to possess a “memory effect”, which is a well-known phenomenon whereby Layered Double Oxides (LDOs)

obtained from dehydration of LDH precursors can reform the original layered structure in contact with water and appropriate anions.<sup>[1]</sup> Using this property, half of the oxygen atoms of the hydroxide groups in the final LDH products can be  $^{17}\text{O}$  labeled if  $^{17}\text{O}$  enriched  $\text{H}_2\text{O}$  is used during the LDO hydration:

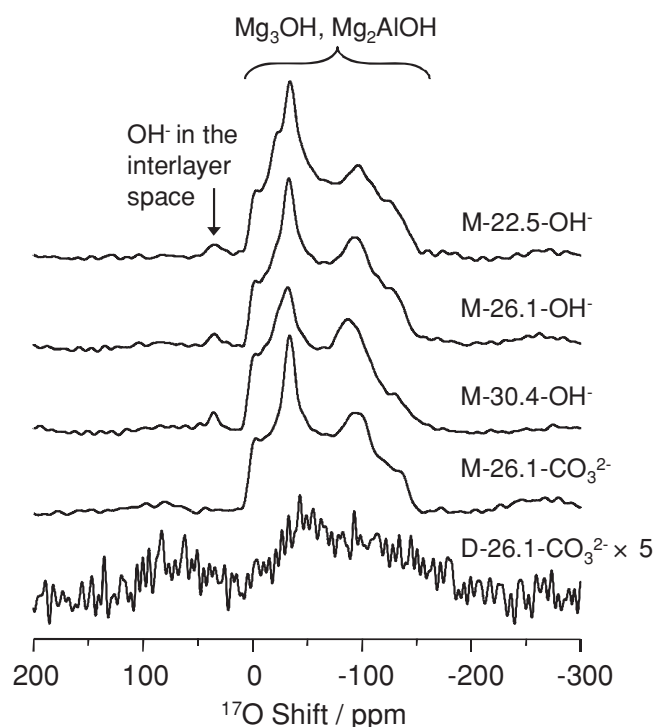
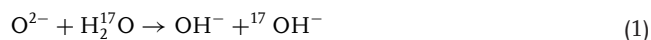


**Figure 2.**  $^{17}\text{O}$  MAS NMR spectra of  $^{17}\text{O}$  enriched LDHs at different Al mole percentages and interlayer species obtained at 9.4 T under MAS frequency of 20 kHz. Each spectrum took about 2.5 h.



Hence, this “memory effect” should provide an efficient and relatively general method to prepare  $^{17}\text{O}$  enriched LDHs (except the rare case where only co-precipitation method generates desired LDH materials). TGA analysis was first performed to identify the minimum temperature required to decompose the LDHs (Figure S2, Supporting Information).<sup>[1,9]</sup> Two transitions of weight loss can be observed in the thermal behavior of LDHs. The first transition ranges from  $\approx 80$  to  $\approx 220$  °C, corresponding to the loss of the interlayer water species, while the second transition from  $\approx 350$  to  $\approx 500$  °C, due to the loss of the hydroxyl groups and anions ( $\text{CO}_3^{2-}$ ).<sup>[1]</sup> Higher temperature is beneficial for the complete decomposition of the anions and the formation of LDOs, however, the reconstruction of the original LDHs structure can be hindered if too high temperatures are used. According to the TGA data, 500 °C was chosen to obtain the LDO precursors for reconstructed LDHs. The XRD patterns of LDOs with different Al mole percentages are shown in Figure S4, Supporting Information.

Several different LDHs with different interlayer species ( $\text{OH}^-$  and  $\text{CO}_3^{2-}$ ) and Al mole percentages ( $[\text{Al}]/([\text{Al}]+[\text{Mg}]) = 22.5, 26.1, 30.4\%$ ) were prepared using the structural “memory effect”. The XRD patterns of reconstructed LDHs (Figure 3) suggest that the crystallinity is comparable to that of the original structures and the diffraction peaks fit well to those of the LDH structure without other unwanted phases. While a fraction of the Al cations in LDO are in the 4-coordinated environment, leading to resonances at 60–85 ppm in  $^{27}\text{Al}$  NMR,<sup>[3,8]</sup> only a sharp peak at  $\approx 9$  ppm corresponding to 6-coordinated Al can be observed in the reconstructed LDH materials (Figure S5, Supporting Information). This indicates that the reconstruction process was complete.

The single pulse  $^{17}\text{O}$  MAS NMR spectra of all four  $^{17}\text{O}$  enriched LDHs obtained with the “memory effect” route are shown in Figure 2, and show very good S/N demonstrating that this route is highly efficient for  $^{17}\text{O}$  enrichment. All  $^{17}\text{O}$  spectra

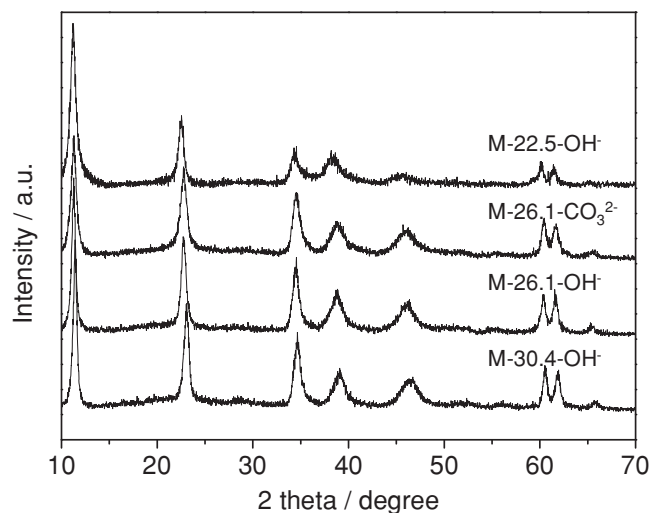


**Figure 3.** Powder XRD patterns of  $^{17}\text{O}$ -enriched LDHs samples prepared via the “memory effect”.

of LDHs contain a broad peak around 10 to  $\sim 180$  ppm, in which characteristic second order quadrupolar line shapes with a non-zero asymmetry parameter could be distinguished. A small but relatively narrow peak at approximately 40 ppm was also observed for all LDHs with  $\text{OH}^-$  in the interlayer spaces but not in the  $\text{CO}_3^{2-}$ -containing LDH sample suggesting that this resonance arises from  $\text{OH}^-$  in the interlayers. The amount of  $\text{OH}^-$  anions observed by  $^{17}\text{O}$  NMR is small due to rapid exchange with water in the air (see Supporting Information for further discussion).

The residual broadenings observed in Figure 2 could be removed in two-dimensional multiple quantum MAS (MQMAS) experiments (Figure 4).<sup>[21,22]</sup> In such experiment, by correlating single quantum coherence and multiple quantum coherence, high resolution spectra without additional broadening due to the second-order quadrupolar interaction can be obtained in the isotropic dimension. Two different oxygen environments could be clearly resolved at  $\delta_{\text{H}} = 53.0$  and 64.8 ppm in the isotropic dimension (Figure 5a), the ratio of the intensities of the two peaks depending on the Al mole percentage. Line shape simulation of slices extracted parallel to the anisotropic dimension (with broadening from the second-order quadrupolar interaction) (Figures 4a,b) gives the NMR parameters (quadrupolar coupling constant,  $C_Q$ , which measures the strength of the quadrupolar interaction, and asymmetry parameter,  $\eta$ , which measures the deviation of the EFG from axial symmetry) relevant to each site (Table 1).

The parameters of the  $\delta_{\text{H}} = 53.0$  ppm resonance are similar to those of the related brucite  $\text{Mg}(\text{OH})_2$  mineral<sup>[23]</sup> and this resonance is therefore assigned to the oxygen atoms in  $\text{Mg}_3\text{OH}$  environments in an LDH (Figure 1c). The asymmetry parameter  $\eta$  is equal to 0, consistent with the fact that the oxygen ions at  $\text{Mg}_3\text{OH}$  sites are in an axial environment with a  $C_3$  rotational axis. The second resonance observed at  $\delta_{\text{H}} = 64.8$  ppm is assigned to the  $\text{Mg}_2\text{AlOH}$  sites (Figure 1c) on the basis of the extracted  $\eta$  value of 0.3 (Table 1), which indicates that the oxygen environment is distorted from axial symmetry.

Ab initio calculations have been performed for hydroxide-like clusters  $\text{Mg}_{12}(\text{OH})_{25}^-$  and  $\text{Mg}_{11}\text{Al}(\text{OH})_{25}$ , corresponding to  $\text{Mg}_3\text{OH}$  and  $\text{Mg}_2\text{AlOH}$  environments, respectively, to support the spectral assignment (Table S2 and Figure S6, Supporting Information). The computed values of  $\eta$  in  $\text{Mg}_3\text{OH}$  are all very close to 0, consistent with the  $C_3$  symmetry while the values of  $\eta$  predicted for  $\text{Mg}_2\text{AlOH}$  range from 0.45–0.46, only slightly larger than the experimental value of 0.3. The calculations also predict that the quadrupolar coupling constant  $C_Q$  for  $\text{Mg}_3\text{OH}$  and  $\text{Mg}_2\text{AlOH}$  range from 7.0–7.5 and 6.5–7.0 MHz, respectively, in reasonable agreement with experimental values (Table 1 and Table S2, Supporting Information). The calculated values are all slightly larger than the values measured at room temperature, in agreement with previous  $^{17}\text{O}$  NMR calculations of zeolitic clusters.<sup>[20,24,25]</sup> The small differences between the experimental results and calculations may also come from the fact that the interlayer anions and water molecules are not included in these calculations.

The isotropic projections obtained from  $^{17}\text{O}$  MQMAS data show much higher resolution compared to the  $^1\text{H}$  NMR spectra of non-enriched  $\text{OH}^-$  anion-containing LDHs under ultrafast MAS (Figure 6a), while at this fast spinning rate, different H

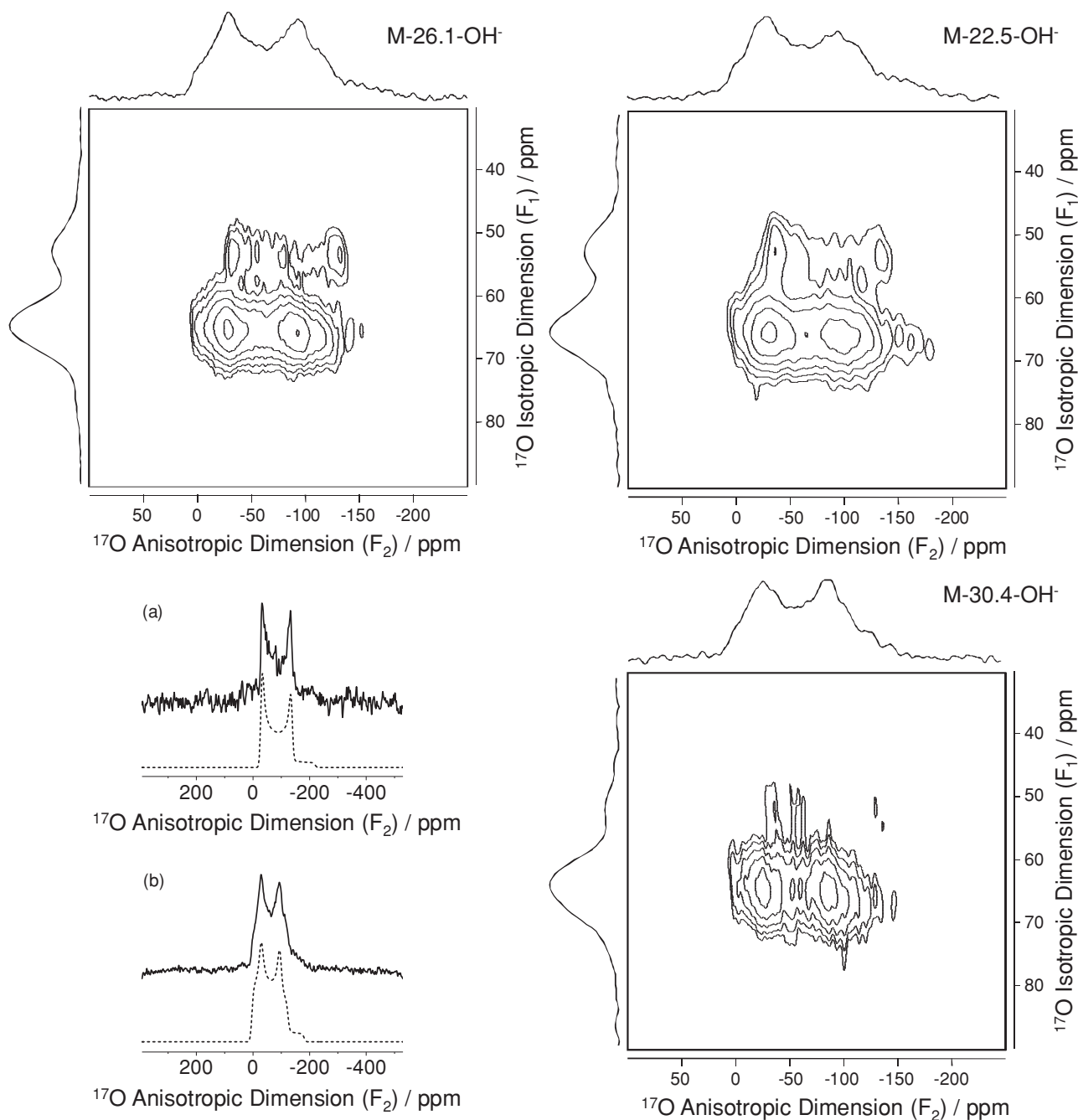


**Figure 4.**  $^{17}\text{O}$  3QMAS NMR spectra of LDHs at 9.4 T under MAS frequency of 23 kHz. Projections of the anisotropic and isotropic dimensions are shown on the top and left side of the 2D spectrum, respectively. Cross sections (full lines) extracted parallel to anisotropic dimension of the 2D 3Q MAS spectrum for M-26.1- $\text{OH}^-$  at a) 53.0 and b) 64.8 ppm in  $F_1$  along with the best fit simulation (dotted lines) using the parameters presented in Table 1. The time to finish each 2D spectrum ranges from 16 to 72 hours.

species ( $\text{H}_2\text{O}$ ,  $\text{Mg}_2\text{AlOH}$  and  $\text{Mg}_3\text{OH}$ ) in  $\text{NO}_3^-$ -containing LDHs can be resolved in  $^1\text{H}$  NMR (Figure 6b). It suggests that the lower  $^1\text{H}$  NMR resolution associated with  $\text{OH}^-$  anion-containing LDHs is due to the presence of more chemically distinct H-containing species, the greater  $^1\text{H}$ - $^1\text{H}$  homonuclear dipolar coupling present and/or more complicated dynamics. Compared to the  $^1\text{H}$  ultrafast MAS NMR approach, only an intermediate spinning speed is used ( $\approx 20$  kHz) for  $^{17}\text{O}$  MAS

NMR. At this spinning rate, dipolar recoupling techniques (e.g., cross polarization (CP), see Figures S7,S8 and other Supporting Information) can be more easily incorporated to study the interactions in LDHs, compared to the ultrafast spinning condition. The comparison clearly shows the enormous advantage of applying  $^{17}\text{O}$  NMR spectroscopy to distinguish the distinct local environments in studying more complicated LDH materials.



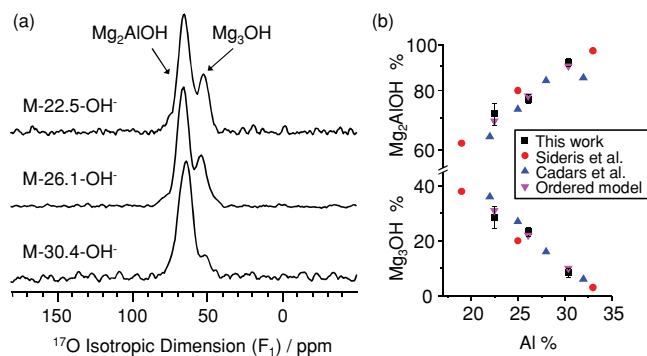


**Figure 5.** a) Isotopic projections of  $^{17}\text{O}$  3QMAS spectra of  $^{17}\text{O}$  enriched LDHs with  $\text{OH}^-$  in the interlayer space with different Al mole percentages at 9.4 T. b) The mole percentages of  $\text{Mg}_3\text{OH}$  and  $\text{Mg}_2\text{AlOH}$  environments in comparison with previous work using  $^{25}\text{Mg}$ <sup>[14,15]</sup> and  $^1\text{H}$ <sup>[13–15]</sup> NMR, and predictions using a model that assumes that no Al–O–Al linkages are formed.

The 1D isotropic spectra obtained from the 3QMAS spectra for the  $\text{OH}^-$  anion-containing LDHs show that the relative concentration of the  $\text{Mg}_3\text{OH}$  environments increase when the Al mole percentage decreases. The data were fit to give the ratios of the  $\text{Mg}_3\text{OH}/\text{Mg}_2\text{AlOH}$  (Figure S9 and Table S3, Supporting Information). The values of the quadrupolar product  $P_Q = C_Q(1+\eta^2/3)^{1/2}$  are very similar (a difference of <5%) for the two oxygen environments, leading to negligible differences in the MQ excitation efficiencies, therefore the intensities in the isotropic dimension should reflect the quantities directly and no additional correction was made on the intensities.<sup>[26]</sup> Consistent with this assertion, the  $^{17}\text{O}$  single pulse NMR data can also be well fit with these  $\text{Mg}_3\text{OH}/\text{Mg}_2\text{AlOH}$  ratios and the NMR parameters in Table 1 (Figure S10, Supporting Information). The mole percentages of  $\text{Mg}_3\text{OH}$  and  $\text{Mg}_2\text{AlOH}$  sites in the hydroxide layers of  $\text{OH}^-$  anion-containing LDHs extracted from the  $^{17}\text{O}$  NMR data are in good agreement with the predictions made assuming cation ordering with Al–O–Al linkage avoidance and thus the results from  $^{25}\text{Mg}$  NMR and  $^1\text{H}$  NMR<sup>[14,15]</sup> investigations of  $\text{NO}_3^-$ -containing LDHs (Figure 5b). No  $\text{MgAl}_2\text{OH}$  environment was observed and a different trend in the percentage of  $\text{Mg}_2\text{AlOH}$  was found in our study compared to the results from Cadars and co-workers<sup>[13]</sup> at high Al mole percentages (>30%), again we believe their observation of the Al–O–Al defects originates from the different preparation methods.<sup>[14]</sup>

The weak signal ascribed to  $\text{OH}^-$  in the interlayer spaces for M-26.1- $\text{OH}^-$  was not observed in the 3QMAS spectrum at 9.4 T but could be successfully detected at 16.4 T (Figure S11, Supporting Information). The  $P_Q$  value (obtained from the peak

**Table 1.**  $^{17}\text{O}$  NMR parameters of the  $\text{Mg}_3\text{OH}$  and  $\text{Mg}_2\text{AlOH}$  oxygen sites in the hydroxide layers of the LDHs structure.

Site	$\delta_i$	$\delta_{\text{CS}}$	$C_Q$ [MHz]	$\eta$	$P_Q$ [MHz] <sup>a)</sup>
$\text{Mg}_3\text{OH}$	53.0(5)	2.5(5)	6.6(1)	0.0(1)	6.6(1)
$\text{Mg}_2\text{AlOH}$	64.8(5)	18.0(5)	6.2(1)	0.3(1)	6.3(2)

<sup>a)</sup> Calculated as  $C_Q(1+\eta^2/3)^{1/2}$ .

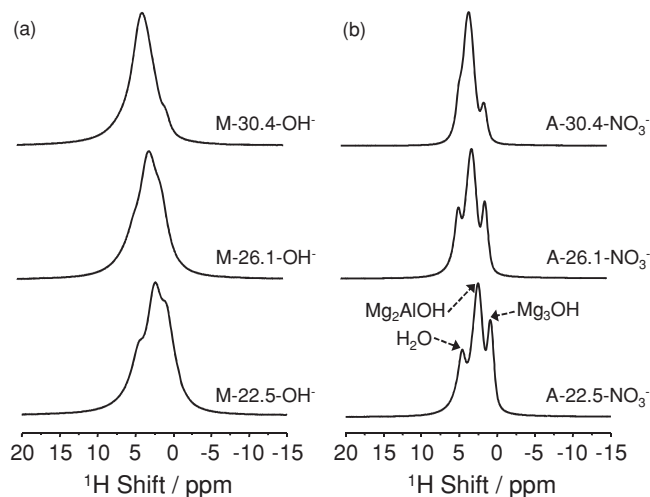


**Figure 6.** A comparison of the  $^1\text{H}$  MAS NMR spectra of Mg and Al containing a) LDHs with  $\text{OH}^-$  in the interlayer spaces (non-enriched) and b) the corresponding  $\text{NO}_3^-$ -containing LDHs, for different Al mole percentages (22.5, 26.1, and 30.4%). Spectra were acquired at a spinning rate of 60 kHz at 9.4 T.

position of the 3QMAS resonance in the high field spectra) and thus quadrupolar coupling constant for the  $\text{OH}^-$  anions in the interlayer regions is much smaller than those of the framework  $\text{Mg}_3\text{OH}$  and  $\text{Mg}_2\text{AlOH}$  sites. This is tentatively ascribed to the more ionic nature of the interlayer  $\text{OH}^-$  species in comparison to the framework oxygen sites.<sup>[27]</sup> The much smaller quadrupolar coupling is believed to be associated with the low efficiency in detecting this species in the 3QMAS and CP-MAS experiments, in which the experimental parameters were optimized for the major  $\text{OH}^-$  species ( $\text{Mg}_3\text{OH}/\text{Mg}_2\text{AlOH}$ ) with much larger  $C_Q$ .

### 3. Conclusions

An efficient  $^{17}\text{O}$  enrichment method based on the “memory effect” of LDHs has been demonstrated. The method uses only a very small amount of  $^{17}\text{O}$ -enriched water and allows  $^{17}\text{O}$  NMR spectra to be readily obtained for a variety of LDHs. Both  $\text{Mg}_3\text{OH}$  and  $\text{Mg}_2\text{AlOH}$  environments could be observed with parameters consistent with ab initio calculations. The intensities of these two sites in LDHs with hydroxide ions as the interlayer species can be quantitatively determined and the results agree well with the Al–O–Al avoidance model demonstrated previously by  $^1\text{H}$  and  $^{25}\text{Mg}$  NMR for  $\text{NO}_3^-$ -containing LDHs. The resolution of the signals of the different  $\text{M}_3^{17}\text{OH}$  local environments is better than the  $^1\text{H}$  signals of the same species obtained by ultrafast MAS NMR spectroscopy. Further local structural information can be obtained by using a variety of dipolar recoupling schemes without the need for fast MAS and high external field strengths. Extension of this approach to study the structure of a wider range of LDHs and to explore the key interactions and applications associated with their supra-molecular chemistry can be readily envisaged.

## 4. Experimental Section

**The  $\text{CO}_3^{2-}$  and  $\text{NO}_3^-$ -Containing LDH Materials:** The starting MgAl-LDH materials with  $\text{CO}_3^{2-}$  anions in the interlayer spaces with different levels of Al substitution were synthesized by a conventional co-precipitation method followed by ion exchange.<sup>[28]</sup> In a typical synthesis, stoichiometric amounts of  $\text{Mg}(\text{NO}_3)_2 \cdot 6\text{H}_2\text{O}$  (Beijing Chemicals,  $\geq 98\%$ ) and  $\text{Al}(\text{NO}_3)_3 \cdot 9\text{H}_2\text{O}$  (Beijing Chemicals,  $\geq 98\%$ ) were dissolved in distilled water ( $[\text{Mg}^{2+}] + [\text{Al}^{3+}] = 1 \text{ M}$ ) to achieve the desired Mg/Al ratio. This solution and 2 M NaOH (Beijing Chemicals,  $\geq 98\%$ ) aqueous solution were then added drop wise at a rate of  $1 \text{ mL min}^{-1}$  at room temperature into a beaker, maintaining a constant pH of 10 by adding either a 2 M  $\text{HNO}_3$  (Beijing Chemicals,  $\geq 98\%$ ) or NaOH solution. After complete precipitation, the obtained gel was refluxed gently at  $80^\circ\text{C}$  for 10 h, and the precipitates were transferred to a 100 mL Teflon Parr hydrothermal autoclave and heated at  $180^\circ\text{C}$  for 36 h. The resulting samples were washed with distilled water and dried overnight at  $80^\circ\text{C}$  to obtain  $\text{NO}_3^-$ -containing LDHs. The as-synthesized LDH- $\text{NO}_3^-$  materials were then mixed with 150 mL of 0.01 M  $\text{Na}_2\text{CO}_3$  (Beijing Chemicals,  $\geq 98\%$ ) aqueous solution and heated at  $100^\circ\text{C}$  for 2 h for ion exchange. The ion exchange process was repeated twice and the products were washed and dried overnight at  $80^\circ\text{C}$  yielding the as-synthesized  $\text{CO}_3^{2-}$ -containing LDHs. The as-prepared LDHs are labeled A-22.5- $\text{NO}_3^-$ , A-26.1- $\text{NO}_3^-$ , A-30.4- $\text{NO}_3^-$ , A-22.5- $\text{CO}_3^{2-}$ , A-26.1- $\text{CO}_3^{2-}$ , and A-30.4- $\text{CO}_3^{2-}$ , respectively, according to the Al mole percentages and the interlayer species.

**$^{17}\text{O}$  Enriched LDHs with Direct Approach:**  $^{17}\text{O}$ -labeled LDHs were prepared by mixing  $^{17}\text{O}$ -enriched water with LDHs directly. In a typical procedure,  $\text{CO}_3^{2-}$ -containing LDH (26.1% Al, 120 mg) was mixed with 20%  $^{17}\text{O}$  enriched  $\text{H}_2\text{O}$  ( $\approx 0.5 \text{ mL}$ , Cambridge Isotope Laboratory) and the mixture was stirred at ambient temperature for 6 days. The resulting product was heated at  $70^\circ\text{C}$  for 8 h to dryness and subsequently denoted "D-26.1- $\text{CO}_3^{2-}$ ". In an alternative procedure,  $\text{CO}_3^{2-}$ -containing LDH (26.1% Al, 120 mg) was mixed with 20%  $^{17}\text{O}$  enriched  $\text{H}_2\text{O}$  ( $\approx 0.5 \text{ mL}$ , Cambridge Isotope Laboratory) in a 15 mL Teflon Parr hydrothermal autoclave and heated at  $90^\circ\text{C}$  for 24 h. The obtained sample was then exposed to air and no precaution was taken to keep the sample away from atm environment. This sample was used to track the exchange between the physisorbed and interlayer water molecules and water molecules in air and designated as "D-26.1- $\text{CO}_3^{2-}$ -wet".

**$^{17}\text{O}$  Enriched LDHs via "Memory Effect":**  $^{17}\text{O}$ -labeled LDHs were prepared by converting the starting LDHs to LDOs followed by regenerating the LDHs structure in different conditions.<sup>[1]</sup> LDOs were obtained by heating the LDHs at  $500^\circ\text{C}$  for 5 h.<sup>[1]</sup>  $^{17}\text{O}$  enriched  $\text{CO}_3^{2-}$ -containing LDH (Al% = 26.1%) was obtained by stirring LDO (160 mg),  $\text{Na}_2\text{CO}_3$  (50 mg) and 20%  $^{17}\text{O}$  enriched  $\text{H}_2\text{O}$  ( $\approx 1 \text{ mL}$ , Cambridge Isotope Laboratory) for 5 days. The product was washed with distilled water ( $\approx 20 \text{ mL}$ ) and the precipitate was dried at  $70^\circ\text{C}$  for 8 h (material denoted as "M-26.1- $\text{CO}_3^{2-}$ ").  $^{17}\text{O}$  enriched LDHs with  $\text{OH}^-$  in the interlayer regions were obtained by hydrothermal treatment. In a typical experiment, 160 mg LDO was placed in a 10 mL crucible inside a 100 mL Teflon Parr hydrothermal autoclave. 0.3 mL  $^{17}\text{O}$  enriched water (20%) was added outside the crucible but inside the autoclave before the system was heated at  $100^\circ\text{C}$  for 9 d. Finally the products were dried  $70^\circ\text{C}$  for 8 h and denoted as "M-22.5- $\text{OH}^-$ ", "M-26.1- $\text{OH}^-$ ", and "M-30.4- $\text{OH}^-$ ", respectively, for the materials with Al mole percentages of 22.5, 26.1, and 30.4%. Due to  $\text{CO}_2$  dissolved in water, there are a small amount of  $\text{CO}_3^{2-}$  and/or  $\text{HCO}_3^-$  in the interlayer spaces in these LDHs.

**Solid-State NMR Spectroscopy:** MAS NMR experiments at a moderate spinning rate were carried out on 9.4 and 16.4 T wide bore Bruker Avance III spectrometers equipped with a 3.2 mm HXY probehead (in double resonance mode). All samples were packed inside 3.2 mm MAS zirconia rotors and spun at  $\nu_r = 20\text{--}23 \text{ kHz}$ .  $^{17}\text{O}$  one-dimensional spectra were recorded at 9.4 T using single pulse experiments and 0.4  $\mu\text{s}$  pulse widths at a radio frequency field amplitude of  $\nu_1 = 70 \text{ kHz}$  (measured on tap water). Two-dimensional triple-quantum MAS NMR experiments were performed at 9.4 and 16.4 T using the z-filtered pulse

sequence.<sup>[21]</sup> Hard and soft pulses were performed at  $\nu_1 = 110 \text{ kHz}$  and approximately 20 kHz, respectively. The multiple-quantum transfer was optimized to increase the excitation efficiency of the MQ coherences. The  $t_1$  increment was rotor-synchronized to one rotor period of 43.48  $\mu\text{s}$  at  $\nu_r = 23 \text{ kHz}$ . Two-pulse phase modulated (TPPM)<sup>[29]</sup>  $^1\text{H}$  decoupling was applied during  $t_1$ -evolution and  $t_2$ -acquisition. The recycle delay was set to 0.4 s for all single pulse and MQMAS experiments. The CP MAS NMR experiments were performed with a MAS rate of 20 kHz and the Hartmann-Hahn condition was set by using the  $^{17}\text{O}$ -enriched LDH sample itself.  $^{17}\text{O}$  and  $^{27}\text{Al}$  chemical shifts were externally referenced to tap water and 0.1 M  $\text{Al}(\text{NO}_3)_3$  aqueous solution, respectively, at 0.0 ppm. NMR line shape simulations were performed with Wsolsids.<sup>[30]</sup>  $^1\text{H}$  ultrafast MAS NMR experiments were carried out at a 9.4 T wide bore Bruker Avance III spectrometer equipped with a 1.3 mm HX probehead. All samples were packed inside 1.3 mm MAS zirconia rotors and spun at  $\nu_r = 60 \text{ kHz}$ .  $^1\text{H}$  MAS spectra were recorded using single pulse experiments and 2  $\mu\text{s}$  pulse widths at a radio frequency field amplitude of  $\nu_1 = 125 \text{ kHz}$ .  $^1\text{H}$  chemical shifts were externally referenced to water at 4.8 ppm.

**Other Characterization:** Powder XRD measurements were performed with a Philips X'Pert Pro X-ray diffractometer with Cu K $\alpha$  radiation ( $\lambda = 1.54184 \text{ \AA}$ , 40 kV and 40 mA). Data were collected between  $10^\circ$  and  $70^\circ$  ( $2\theta$ ), with a step size of  $0.02^\circ$  and a counting time of 0.2 seconds per step. Thermogravimetric analyses were carried out on a NETZSCH STA-449C thermal analysis system. The samples were heated at a rate of  $5 \text{ K min}^{-1}$  from room temperature to  $680^\circ\text{C}$  under ambient atmosphere. ICP spectroscopy was performed with a J-A00 spectrometer (Jarrell-Ash) after samples were digested in 5%  $\text{HNO}_3$ .

**Ab Initio Calculations:** All calculations of the electric field gradient (EFG) were performed using Gaussian 09. Hartree-Fock and Density Functional Theory with hybrid functionals (B3LYP, BLYP and M06) with a 6-311++G (2df, 2p) basis set were selected to calculate the EFG of the central oxygen in the cluster truncated from an LDH crystal. We chose a cluster model that was found to be accurate enough to evaluate the EFG tensor,<sup>[25,31]</sup> and reproduce the real system. A sufficiently large radius of 5.5  $\text{\AA}$  was utilized with respect to the truncated cluster and the corresponding chemical formulae are  $\text{Mg}_{12}(\text{OH})_{25}^-$  and  $\text{Mg}_{11}\text{Al}(\text{OH})_{25}$ , respectively, for the calculations of the oxygen ions in the  $\text{Mg}_3\text{OH}$  and  $\text{Mg}_2\text{AlOH}$  environments. The interlayer anions and water molecules are not included in the calculations. Before calculating the EFG of the truncated clusters, the hydrogen atoms are first added to saturate the valence of the oxygen atoms in the clusters, then the hydrogen atoms are relaxed at the B3LYP/6-311++G(d,p) level of theory with all of the heavy atoms being fixed. When computing the EFG of the center oxygen atoms with the methods mentioned above, a larger basis set of 6-311++G(2df, 2p) is applied. The following EFG tensor convention was used:

$$C_Q = eV_{zz}Q/h$$

$$\eta = (V_{xx} - V_{yy})/V_{zz}$$

where  $V_{xx}$ ,  $V_{yy}$ , and  $V_{zz}$  are principal components of the traceless electric field gradient tensor,  $Q$  is the nuclear electric quadrupole moment (for  $^{17}\text{O}$ ,  $Q = -0.02558 \text{ Barn}$ ).<sup>[25,31]</sup>

## Supporting Information

Supporting Information is available from the Wiley Online Library or from the author.

## Acknowledgements

L.Z. and Z.Q. contributed equally to this work. This work was supported by the National Basic Research Program of China (Grant 2013CB934800), the National Natural Science Foundation of China (NSFC) (Grants

21073083, 20903056, and 21222302), NSFC – Royal Society Joint Program (Grant 21111130201), Program for New Century Excellent Talents in University (NCET-10-0483), the Fundamental Research Funds for the Central Universities (Grant 1124020512) and National Science Fund for Talent Training in Basic Science (Grant J1103310). The authors thank Mr. Junjian Miao and Prof. Shuhua Li at Nanjing University for the help with ab initio calculations. L. Z. thanks the Scientific Research Foundation of Graduate School of Nanjing University (Grant 2012CL05). F.B. thanks the EU Marie Curie actions FP7 for an International Incoming Fellowship (Grant 275212).

Received: April 4, 2013

Revised: July 10, 2013

Published online: November 4, 2013

- [1] F. Cavani, F. Triffrò, A. Vaccari, *Catal. Today* **1991**, 11, 173.
- [2] D. G. Evans, X. Duan, *Chem. Commun.* **2006**, 485.
- [3] R. Liang, S. Xu, D. Yan, W. Shi, R. Tian, H. Yan, M. Wei, D. G. Evans, X. Duan, *Adv. Funct. Mater.* **2012**, 22, 4940.
- [4] a) Z. P. Liu, R. Z. Ma, M. Osada, N. Iyi, Y. Ebina, K. Takada, T. Sasaki, *J. Am. Chem. Soc.* **2006**, 128, 4872; b) D. P. Yan, J. Lu, J. Ma, S. H. Qin, M. Wei, D. G. Evans, X. Duan, *Angew. Chem. Int. Ed.* **2011**, 50, 7037; c) D. P. Yan, J. Lu, J. Ma, M. Wei, D. G. Evans, X. Duan, *Angew. Chem. Int. Ed.* **2011**, 50, 720.
- [5] a) B. M. Choudary, S. Madhi, N. S. Chowdari, M. L. Kantam, B. Sreedhar, *J. Am. Chem. Soc.* **2002**, 124, 14127; b) S. Velu, K. Suzuki, M. Okazaki, M. P. Kapoor, T. Osaki, F. Ohashi, *J. Catal.* **2000**, 194, 373.
- [6] K. H. Goh, T. T. Lim, Z. Dong, *Water Res.* **2008**, 42, 1343.
- [7] H. T. Zhao, K. L. Nagy, *J. Colloid Interface Sci.* **2004**, 274, 613.
- [8] C. Chen, P. Gunawan, X. W. D. Lou, R. Xu, *Adv. Funct. Mater.* **2012**, 22, 780.
- [9] J. Choy, J. Oh, M. Park, K. Sohn, J. Kim, *Adv. Mater.* **2004**, 16, 1181.
- [10] a) J. H. Choy, J. S. Jung, J. M. Oh, M. Park, J. Jeong, Y. K. Kang, O. J. Han, *Biomaterials* **2004**, 25, 3059; b) M. Darder, M. Lopez-Blanco, P. Aranda, F. Leroux, E. Ruiz-Hitzky, *Chem. Mater.* **2005**, 17, 1969.
- [11] a) F. Malherbe, J. P. Besse, *J. Solid State Chem.* **2000**, 155, 332; b) V. Rives, M. a. Angeles Ulibarri, *Coord. Chem. Rev.* **1999**, 181, 61.
- [12] a) S. Britto, P. V. Kamath, *Inorg. Chem.* **2009**, 48, 11646; b) S. Britto, P. V. Kamath, *Inorg. Chem.* **2010**, 49, 11370; c) S. Britto, P. V. Kamath, *Inorg. Chem.* **2011**, 50, 5619.
- [13] S. Cadars, G. Layrac, C. Gérardin, M. Deschamps, J. R. Yates, D. Tichit, D. Massiot, *Chem. Mater.* **2011**, 23, 2821.
- [14] P. J. Sideris, F. Blanc, Z. H. Gan, C. P. Grey, *Chem. Mater.* **2012**, 24, 2449.
- [15] P. J. Sideris, U. G. Nielsen, Z. Gan, C. P. Grey, *Science* **2008**, 321, 113.
- [16] J. Rocha, M. del Arco, V. Rives, M. A. Ulibarri, *J. Mater. Chem.* **1999**, 9, 2499.
- [17] J. P. Yesinowski, H. Eckert, G. R. Rossman, *J. Am. Chem. Soc.* **1988**, 110, 1367.
- [18] A. Lesage, *Phys. Chem. Chem. Phys.* **2009**, 11, 6876.
- [19] a) S. E. Ashbrook, M. E. Smith, *Chem. Soc. Rev.* **2006**, 35, 718; b) C. P. Grey, in *Handbook of Zeolite Science and Technology* (Eds: S. M. Auerbach, K. A. Carrado, P. K. Dutta), Marcel Dekker, New York **2003**, 205.
- [20] J. M. Griffin, L. Clark, V. R. Seymour, D. W. Aldous, D. M. Dawson, D. Iuga, R. E. Morris, S. E. Ashbrook, *Chem. Sci.* **2012**, 3, 2293.
- [21] J. P. Amoureux, C. Fernandez, S. Steuernagel, *J. Magn. Reson., Ser A* **1996**, 123, 116.
- [22] a) L. Frydman, J. S. Harwood, *J. Am. Chem. Soc.* **1995**, 117, 5367; b) A. Medek, J. S. Harwood, L. Frydman, *J. Am. Chem. Soc.* **1995**, 117, 12779.
- [23] E. R. H. van Eck, M. E. Smith, *J. Chem. Phys.* **1998**, 108, 5904.
- [24] L. Peng, H. Huo, Y. Liu, C. P. Grey, *J. Am. Chem. Soc.* **2007**, 129, 335.
- [25] L. M. Peng, Y. Liu, N. J. Kim, J. E. Readman, C. P. Grey, *Nat. Mater.* **2005**, 4, 216.
- [26] a) L. S. Du, J. F. Stebbins, *J. Phys. Chem. B* **2006**, 110, 12427; b) L. M. Peng, J. F. Stebbins, *J. Non-Cryst. Solids* **2007**, 353, 4732.
- [27] H. K. C. Timken, S. E. Schramm, R. J. Kirkpatrick, E. Oldfield, *J. Phys. Chem.* **1987**, 91, 1054.
- [28] a) R. Llamas, C. Jiménez-Sanchidrián, J. R. Ruiz, *Tetrahedron* **2007**, 63, 1435; b) F. Prinetto, D. Tichit, R. Teissier, B. Coq, *Catal. Today* **2000**, 55, 103; c) A. Tsujimura, M. Uchida, A. Okuwaki, *J. Hazard. Mater.* **2007**, 143, 582.
- [29] A. E. Bennett, C. M. Rienstra, M. Auger, K. V. Lakshmi, R. G. Griffin, *J. Chem. Phys.* **1995**, 103, 6951.
- [30] K. Eichele, R. E. Wasylshen, Dalhousie University, Halifax, Canada **2001**.
- [31] a) A. Sutrisno, C. Lu, R. H. Lipson, Y. Huang, *J. Phys. Chem. C* **2009**, 113, 21196; b) A. Wong, R. Ida, X. Mo, Z. Gan, J. Poh, G. Wu, *J. Phys. Chem. A* **2006**, 110, 10084; c) J. Zhu, A. J. Geris, G. Wu, *PCCP* **2009**, 11, 6972.